ELSEVIER

Polymer 43 (2002) 1399–1405

polymer

www.elsevier.com/locate/polymer

Three phase model in drawn thermoplastic polyesters: comparison of differential scanning calorimetry and thermally stimulated depolarisation current experiments

M. Kattan[a,b], E. Dargent[a,*], J. Grenet[a]

[a]*Laboratoire d'Etude et de Caractérisation des Amorphes et des Polymères, Faculté des Sciences, Université de Rouen, 76821 Mont-Saint-Aignan Cedex, France*

[b]*AECS Damascus, P.O. Box 6091, Syria*

Received 30 May 2001; received in revised form 3 October 2001; accepted 16 October 2001

Abstract

Differential scanning calorimetry and thermally stimulated depolarisation current measurements are performed to quantify various phases present in amorphous and semi-crystalline polyester samples uniaxially drawn above their respective glass transition temperature. Results show the appearance of a crystalline phase induced by stretching and of a part of the amorphous phase which does not participate in glass transition. The existence of this phase—called rigid amorphous phase—is enhanced by the presence of crystallites rather than by the drawing.

Keywords: Poly(ethylene terephthalate); Drawing; Thermally stimulated depolarisation currents

1. Introduction

Semi-crystalline polymer structure is usually explained with a two-phase model. Materials are described without transitional region between crystalline and amorphous regions. When cooling from the melt occurred, a part of the material could crystallise at temperatures depending on the experimental conditions. For the remaining amorphous fraction, departure from the liquid-like state occurs in the glass temperature range. During heating from the glassy state, differential scanning calorimetry (DSC) permits to observe the change in thermal heat capacity at the glass transition defined by $\Delta C_p = [C_{p1} - C_{pg}]_{T=T_g}$, difference of thermal heat capacities between liquid and glassy states. For some semi-crystalline polymers made of weakly flexible chains, the increase of ΔC_p is found to be smaller than it would be expected on the basis of the crystallinity [1,2]. It seems that the deviations are caused by molecules whose mobility is somehow hindered even if they are in the amorphous phase [3,4]. To describe easily such polymers, a three-phase model in which a 'rigid' amorphous fraction is taken into account has been proposed [5]. The third phase of this model is a transitional region located between crystalline and mobile amorphous regions (or undisturbed amorphous regions) [6].

One of the polymers for which the three phase model has successfully described its thermal behaviour is poly(ethylene terephthalate) (PET). The crystallinity rate of PET is low and a wholly amorphous material can be obtained by rapid quenching from the melt while annealing above the glass transition temperature induced a «cold» thermal crystallisation. Some authors [7,8] have shown that during annealing, the rigid amorphous fraction crystallises at temperatures lower than the temperatures usually observed for the mobile amorphous fraction and that annealing reduces the part of the rigid amorphous phase into the samples. Due to uniaxial or biaxial drawing, a crystalline phase could also appear in the amorphous material. Indeed, when PET sheets or films are uniaxially drawn at temperature above the glass transition temperature, it is well established that a strain induced crystalline (SIC) phase and that a fibber texture appear above the critical value for the draw ratio [9]. From X-ray analysis, it has been shown that a strain induced crystalline phase appears in PET with initially a weak crystalline texture. Secondly, for higher values of the draw ratio, the drawing tends to align the crystallites with the drawing direction (rather than to increase the degree of crystallinity). An extra texture where the planes of the phenyl rings are quasi-parallel to the film surface is

* Corresponding author. Tel.: +33-23-514-6881; fax: +33-23-514-6882.
E-mail address: eric.dargent@univ-rouen.fr (E. Dargent).

0032-3861/02/$ - see front matter
PII: S0032-3861(01)00719-4

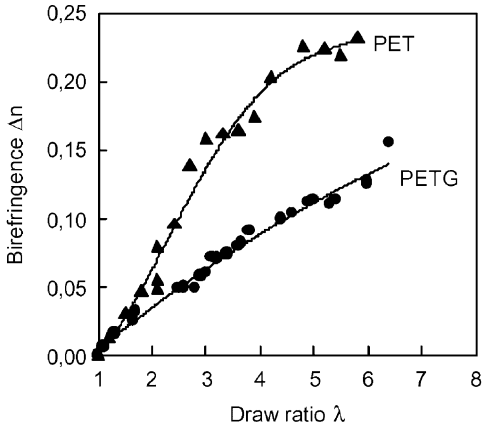

Fig. 1. Birefringence of the uniaxially drawn PET and PETG samples versus the draw ratio λ. Lines are only guides for the eyes.

also observed for the highly drawn sample [10]. However, for drawn materials, it is difficult to separate the respective influence of the crystallisation and of the drawing on the mobility of the amorphous phase. We try to settle this question by comparing drawn PET and copolyester behaviour.

The crystallisation of the PET could be slowed down by replacing some of the ethylene glycol with secondary glycols. With a sufficient amount of cyclohexane-1,4-dimethanol (CHDM) added, poly(ethylene glycol-*co*-cyclohexane-1,4-dimethanol terephthalate) PETG can be obtained. This material industrially used as amorphous copolyester is, in principle, unable to crystallise. Nevertheless, we have shown in a previous work [11] that PETG can also crystallise and that the degree of crystallinity of highly drawn PETG reaches only 3% in mass while it could be as great as 40% for drawn PET. This work is based on the assumption that a description of the structure is possible assuming additivity of properties for the three phases. By thermal analysis, we give the respective percentage of mobile and rigid amorphous phases in these drawn polyesters. This permits us to give new information about the third phase. Thermally stimulated depolarisation currents (TSDC) measurements are used in addition to classical DSC to characterise our materials. Since Van Turnhout's pioneer works [12], TSDC has been frequently employed to investigate the molecular motions in polymeric materials [12–15]. The high interest of TSDC technique is due to the low equivalent frequency of about 10^{-3} Hz [13] and its capability to resolve complex dielectric transitions into narrow distributions of relaxations process [15]. Moreover, the high sensitivity makes TSDC quite useful for the study of main and secondary relaxations in amorphous or semi-crystalline polymers.

2. Experimental

2.1. Materials and sample preparation

PET films ($\bar{M}_n$ of 31,000 g/mol) are isotropic and amorphous judging from birefringence, density and X-ray diffraction measurements. PETG 6763 from Tennessee Eastman Co. is an amorphous copolymer with $\bar{M}_n \cong 26{,}000$ g/mol. PETG consist of cyclohexane dimethanol, ethylene glycol and terephtalic acid with a molar ratio of approximately 1:2:3. Before the drawing period, the samples of PET and PETG are kept in the heating chamber of a tensile machine at 95 °C for 5 min, to allow a homogenous temperature distribution in the films. The sample temperature is controlled by an optical pyrometer. The samples (40×60 mm^2) are uniaxially drawn at a strain rate of 0.14 s^{-1} in the tensile machine. The drawing temperature (95 °C) is chosen between the glass transition temperature and the cold crystallisation temperature of PET to allow homogeneous drawing and to avoid thermal crystallisation. After drawing, the material is cold air-quenched to room temperature in order to freeze-in its structural state. Finally, different samples are cut from the drawn materials and the draw ratio, λ, equal to the ratio of the extended length over the original length, is measured. It was found that λ varied from 1 to 7.2. Samples are stored before experiments under vacuum in the presence of P_2O_5 at 20 °C in order to avoid moisture sorption. For analysis, the samples are about 0.5 mm thick with areas of 150 and 28 mm^2 for TSDC and DSC, respectively.

2.2. Methods

TSDC measurements are performed with an apparatus developed in our laboratory [16]. The sample is subjected to an electric field ($E = 10^6$ V m^{-1}) for a period t_p (2 min) at a polarisation temperature T_p just above its glass transition T_g. The permanent dipoles of the sample, although hindered in their rotations by viscous forces, are gradually orientated by the electric field and a polarisation is in this way created. Then, decrease the temperature down to −150 °C at a constant cooling rate freezes in most of the permanent dipoles. At this temperature, the electric field is cut off and a short circuit is set up. The increase in temperature (at a constant rate $r = 10$ K min^{-1}) allows gradual relaxation of the different polarised units. The decay of the polarisation generates a depolarisation current I. Using this method, complex spectra $I = f(T)$ are obtained which consist of several peaks [12]. Optical anisotropy of samples is measured by birefringence measurements at room temperature and using a spectrophotometric method [17]. Calorimetric investigations are performed with a Perkin Elmer DSC7 calorimeter. Its calibrations in temperature and energy are achieved at 10 K min^{-1} under nitrogen atmosphere using indium and zinc as standards. All the DSC curves presented in the following are normalised to 1 mg of matter.

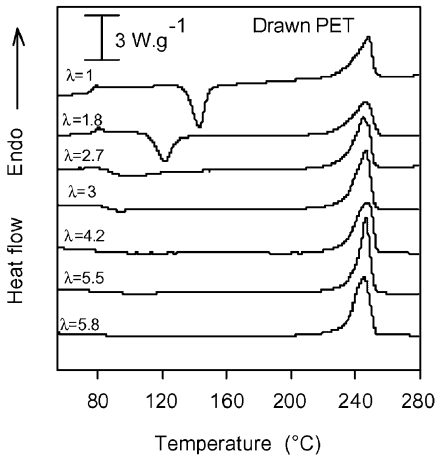

Fig. 2. Normalised DSC curves for various drawn PET samples (the draw ratios are indicated in the figure). The curves are shifted for visibility.

3. Results

3.1. Birefringence studies

Birefringence is due to a difference between the principal refractive indices within a material and its variations can be interpreted with regard to average orientation of the macromolecules. Depending on the authors, the maximum values of Δn proposed in literature for PET lie between 0.212 [18] and 0.290 [19] for the crystalline phase (Δn_c) and between 0.200 [20] and 0.275 [21] for the amorphous phase (Δn_a). The birefringence data are displayed in Fig. 1 and the lines are solely included to facilitate visualisation of changes over the draw ratio (λ). For PET samples, the maximum observed for Δn (0.23) is very close to the values in literature showing that the orientation developed by the drawing has practically reached its maximum for $\lambda > 5$. The weak optical anisotropy of PETG ($\Delta n < 0.15$) is probably due to the presence of CHDM which is not a planar molecular group as the phenylene group. Another work has shown that the maximum value of Δn for uniaxially drawn PCT (in which cyclohexane dimethanol has completely replaced ethylene glycol) is close to 0.10 [22]. The spatial arrangement of CHDM limits the ability of the macromolecule to be included (to be close at least) in a plane containing the drawing direction. Nevertheless, the gradual increase of the birefringence of PETG with λ shows a progressive orientation of the macromolecules in the drawing direction.

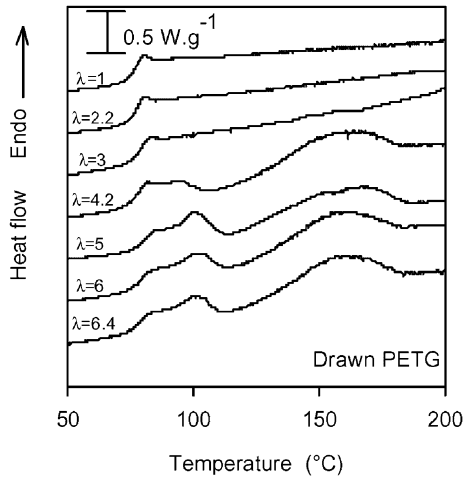

Fig. 3. Normalised DSC curves for various drawn PETG samples (the draw ratios are indicated in the figure). The curves are shifted for visibility.

3.2. Differential scanning calorimetry studies

Fig. 2 ($\lambda = 1$) shows the expected DSC curve for undrawn and amorphous PET. One can notice: (i) the glass transition at 70 °C $< T_g <$ 85 °C, evidenced by the endothermic step, (ii) the thermal cold crystallisation which is observed by the exothermic peak at 130 °C $< T_c <$ 170 °C, (iii) the melting peak of the crystalline phase between 220 and 260 °C which occurs as an endothermic peak. Increase of the draw ratio leads to decrease in the cold crystallisation temperature toward the glass transition one with a concomitant decrease of the crystallisation enthalpy. For draw ratio $\lambda > 4$, the thermal cold crystallisation has completely disappeared because in these cases, the degree of crystallinity of samples have reached its maximum before DSC heating. Analysis of undrawn PETG sample ($\lambda = 1$, Fig. 3) shows the glass transition at 70 $< T_g <$ 85 °C. As for other wholly amorphous thermoplastics, the glass transition is the unique observable thermal phenomenon. Then, DSC scans look similar up to $\lambda = 3.5$ (weakly drawn samples). For highly drawn PETG samples ($\lambda > 3.5$), extra thermal phenomena are observed between 95 and 180 °C. They consist of weak exothermic and endothermic phenomena. From X-ray diffraction and optical microscopy measurements, we have already shown that these thermal phenomena must be attributed to crystallisation and melting of material [11]. For PETG, the variations of heat capacity at the glass transition ΔC_p (derivated from DSC data) are weak and show a quasi-linear decrease with λ (Fig. 4). For PET, ΔC_p shows an important decrease between $\lambda = 2$ and $\lambda = 4$ and then remains practically constant. If the variations of ΔC_p give quantitative information on the evolution of the mobile amorphous phase, variations of the temperature domain of the glass transition show evolution of the amorphous phase homogeneity. Fig. 5 reports the width ΔT_g of the glass transition observable on DSC curves. For PETG, this value is quasi-independent of the draw ratio while for PET, ΔT_g included between 10 and 20 °C for the lowest draw ratios increases with λ up to 35 °C for $\lambda > 6.8$. These results indicate that homogeneity of the amorphous phase of PETG does not depend on the drawing while in PET, the amorphous phase becomes more heterogeneous with increasing λ.

3.3. Thermally stimulated depolarisation currents studies

One of the interests of TSDC experiments is the

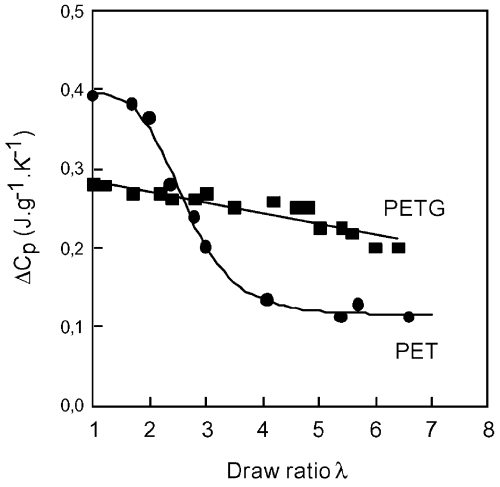

Fig. 4. ΔC_p difference of thermal heat capacities between liquid and glassy states at the T_g mid point glass transition temperature versus the draw ratio λ.

possibility to explore the secondary relaxations which occur at low temperature. Figs. 6 and 7 show the −20 to +120 °C regions while Figs. 8 and 9 show the low temperature regions for PET and PETG, respectively. For undrawn PET, one can observe (Fig. 6) a peak around 70 °C. This peak, called α peak, is the dielectric manifestation of the glass transition. Indeed, we have noted that the temperature of the maximum of the peak, T_α, is equal to the onset of the glass transition observed by DSC and called T_g onset. Although keeping the same shape, the α peak shifts toward higher temperatures and its magnitude decreases when λ increases up to 3.8. For $\lambda > 3.8$, the shape of the α peak becomes different: a first peak is observable at 30 °C and the second at 90 °C. The magnitude of the highest peak (which correspond to the glass transition) is drastically weaker than for the one observed. The lowest peak, also observed for drawn PETG, is generally attributed to localised motion of aromatic cycles of anisotropic polymers [23,24].

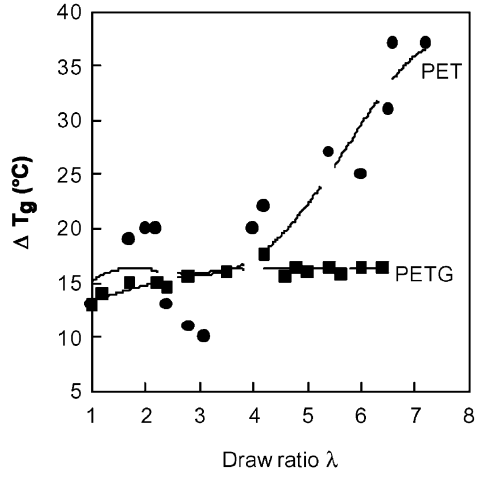

Fig. 5. Width of the glass transition ΔT_g versus the draw ratio λ.

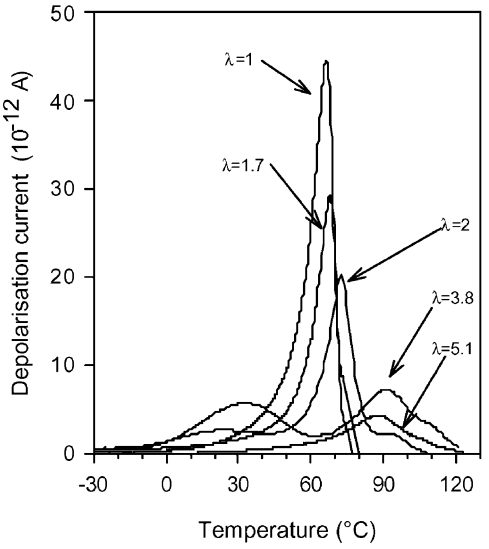

Fig. 6. TSDC curves for different drawn PET (the draw ratios are indicated in the figure). The experimental set of conditions are: the polarisation temperature is just above T_g and the depolarisation temperature is −150 °C, the electric field is 10^6 V m^{-1}, the heating and the cooling rates are 10 °C min^{-1}.

For PETG, the same sequence as for weakly drawn PET is observable (Fig. 7): T_α increases and the peak area decreases with λ. We can note that the TSDC peak of a highly drawn PETG ($\lambda = 6.4$) is comparable in magnitude and temperature to the peak of a $\lambda = 2$ drawn PET. In the low temperature range (Figs. 8 and 9), a large peak of very low magnitude is observed. This peak, called β peak, is attributed to secondary relaxations of dipoles. As for the main α peak, an evolution of the β peak occurs with increasing

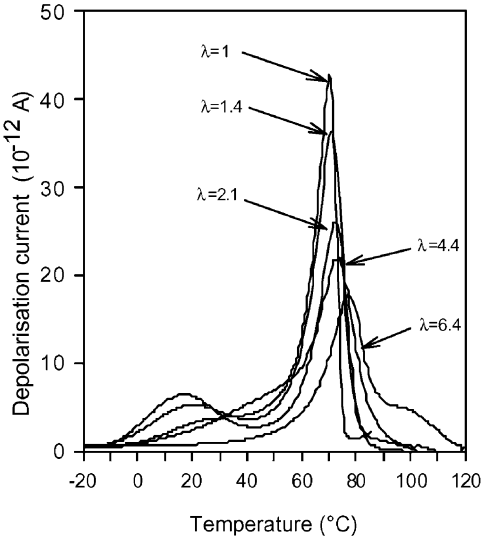

Fig. 7. TSDC curves for different drawn PETG (the draw ratios are indicated in the figure). The experimental set of conditions are: the polarisation temperatures are just above T_g and the depolarisation temperature is −150 °C, the electric field is 10^6 V m^{-1}, the heating and the cooling rates are 10 °C min^{-1}.

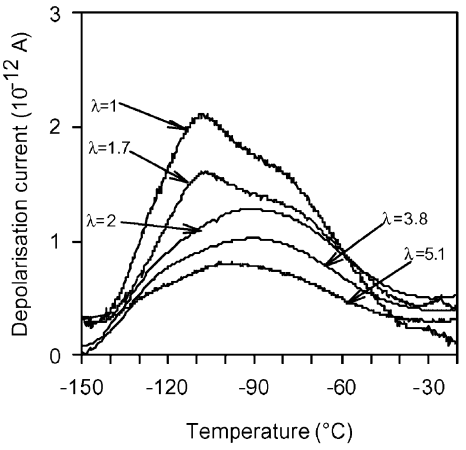

Fig. 8. Low temperatures TSDC curves for different drawn PET (the draw ratios are indicated in the figure). The experimental set of conditions are: the polarisation temperatures are just above T_g and the depolarisation temperature is $-150\,^{\circ}C$, the electric field is $10^6\,V\,m^{-1}$, the heating and the cooling rates are $10\,^{\circ}C\,min^{-1}$.

draw ratio. Due to the important width of these peaks, no significant variation of the temperature of the maximum is observable but the magnitude decreases greatly when λ increases. For PETG, the β peaks have the same shape but do not seem to be modified by the drawing, showing no significant variations of the depolarisation current.

4. Discussion

To quantify the different phases present in the drawn polyesters, we must first calculate the crystallinity induced by the drawing. This degree of crystallinity X_c could be deduced from heating DSC data by the following equation

$$X_c = \frac{\Delta H_f - \Delta H_c}{\Delta H_f^0} \tag{1}$$

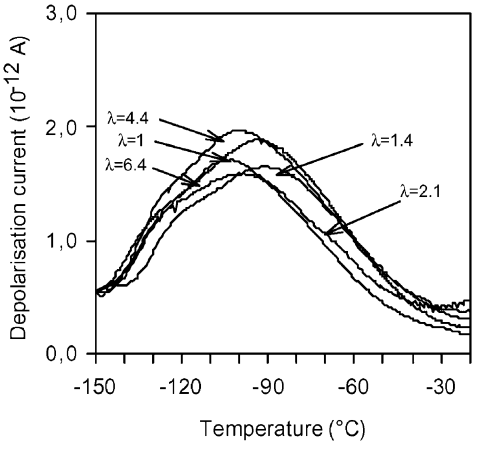

Fig. 9. Low temperature TSDC curves for different drawn PETG (the draw ratios are indicated in the figure). The experimental set of conditions are: the polarisation temperatures are just above T_g and the depolarisation temperature is $-150\,^{\circ}C$, the electric field is $10^6\,V\,m^{-1}$, the heating and the cooling rates are $10\,^{\circ}C\,min^{-1}$.

in which ΔH_f is the measured enthalpy of fusion of any sample, ΔH_f^0 is the calculated enthalpy of fusion of wholly crystalline material ($\Delta H_f^0 = 140\,J/g$ for PET [25] and $\Delta H_f^0 = 88\,J/g$ for PETG [11]) and ΔH_c is the enthalpy of the cold crystallisation observed during the DSC run. Indeed, the experimental enthalpy of fusion ΔH_f corresponds to the fusion of the entire crystal part of samples, i.e. the crystallinity present before the DSC scan and the crystallinity developed during the scan which is measurable by the peak of cold crystallisation. Up to $\lambda = 2$, the initial degree of crystallinity of drawn PET samples is negligible (Fig. 10). Then it raises with λ until $\lambda = 5$. For the highest draw ratio, X_c remains practically constant and close to 40%. For PETG drawn samples, a crystalline phase appears only when the draw ratio becomes greater than $\lambda = 4$ and could reach 3.5% of the mass of the sample for the highest λ. Of course, this difference of crystallinity between PET and PETG is obviously due to the presence of CHDM which limits drastically the ability to crystallise. Classically, it is possible to calculate the degree of amorphous phase X_{am} from the ΔC_p step data at the glass transition

$$X_{am} = \frac{\Delta C_p}{\Delta C_{p0}} \tag{2}$$

where ΔC_p is the jump at T_g of the thermal heat capacity of a drawn sample and ΔC_{p0}, the jump at T_g of the thermal heat capacity of an undrawn and wholly amorphous sample. On the other hand, TSDC can also permit to reach the degree of amorphous phase. If we considered dipoles with a single relaxation time τ, the polarisation created during the charging process satisfies

$$P_s(t) = \frac{N\mu^2}{3kT} E\left[1 - \exp\left(-\frac{t}{\tau}\right)\right] \tag{3}$$

where k is Boltzmann's constant, μ, the dipolar moment of the dipoles and N is the number of dipoles per unit volume [12]. Because of the ideal short-circuit at $-150\,^{\circ}C$, the initial value of the polarisation in the TSDC discharge experiment equals the value of $P_s(t)$ at the end of the charging period. At the end of heating, all retained polarisation have disappeared. In this work, we suppose that the period of polarisation t_p at temperature T_p is sufficiently long to permit to polarisation to reach its saturation value P_0:

$$P_0 = \frac{N\mu^2}{3kT_p} E \tag{4}$$

In this simplistic approach, the polarisation P_0 can be obtained by integrating the depolarisation current curves. Differences between values of P_0 for different drawn samples can be attributed to a variation of the concentration of dipoles N (T_p, E and μ are constants). Assuming that the concentration of mobile dipoles is proportional to the quantity of amorphous phase present in samples, a degree of

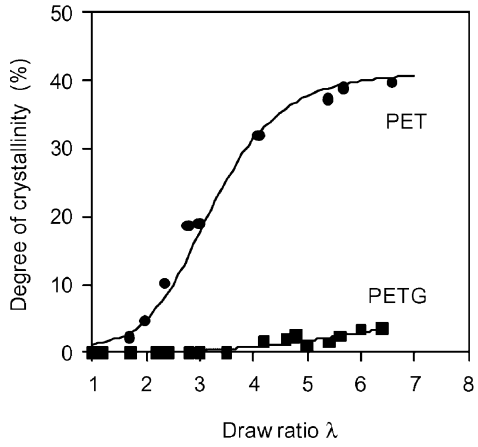

Fig. 10. Degree of crystallinity X_c calculated from Eq. (1) for PET and PETG versus the draw ratio λ.

amorphous phase X'_{am} can be calculated by

$$X'_{am} = P_0/P_{0max} \quad (5)$$

where P_{0max} is the polarisation of an undrawn and wholly amorphous film. In Fig. 11, we have reported the variation of X_{am} and X'_{am} versus λ for both polymers at the glass transition. Although the values of X_{am} and X'_{am} are not identical, their evolutions are similar: for PET, the degree of mobile amorphous phase decreases drastically between $\lambda = 2$ and $\lambda = 5$ while for PETG, the decreases of X_{am} and X'_{am} are weak and quasi-linear. For the β relaxation process (not observable by DSC), it is only possible to calculate X'_{am}; for drawn PET films, X'_{am} decrease with λ between $\lambda = 2.5$ and $\lambda = 5$ while X'_{am} remains practically constant for drawn PETG films (Fig. 12).

The comparison of the respective variations of the degree of crystallinity and the degree of amorphous phase

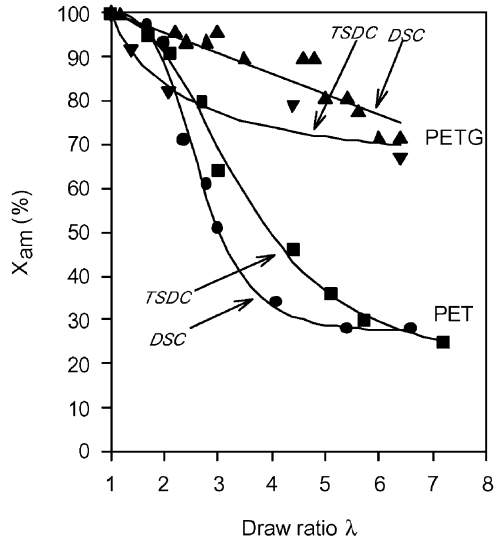

Fig. 11. Evolution with λ of the degrees of amorphous phase X_{am} (Eq. (2)) and X'_{am} (Eq. (4) for the α peak) for drawn PET and PETG.

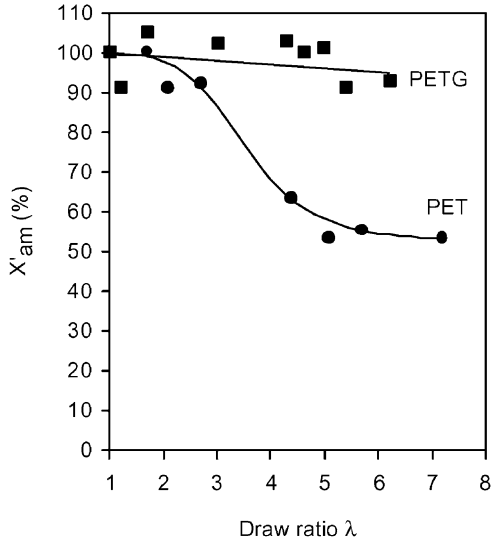

Fig. 12. Evolution with λ of the degree of amorphous phase X'_{am} calculated on the β peak.

(Figs. 10–12) shows that the diminutions of X_{am} and X'_{am} are concomitant with the increase of X_c. This is evident that the appearance of a strain induced crystalline phase decreases the quantity of the remaining amorphous phase. For the β process of drawn PET and PETG, the decrease of X'_{am} can be explained by the increase of X_c (for example PET with $\lambda = 5.7 : X'_{am} = 55\%$ and $X_c = 39\%$ and for PETG with $\lambda = 6.2 : X'_{am} = 93\%$ and $X_c = 3\%$). So, the motions which occur at T_β can be described by a two-phase model in which $X_{am} + X_c = 100$. The temperatures of relaxation are not modified by the drawing and only the dipoles of the crystalline phase do not contribute to the local motion. For the glass transition (i.e. the main α relaxation), the decrease of X_{am} and X'_{am} are more important than the

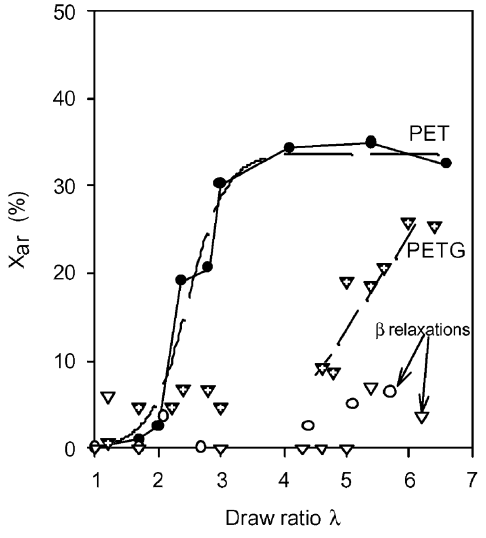

Fig. 13. Percentage of rigid amorphous fraction versus draw ratio for PET and PETG calculated for the glass transition (●: PET, ▼: PETG) and for the β peak (○: PET, ▽: PETG).

increase of X_c (for example PET with $\lambda = 6.6 : X_{am} = 28\%$ and $X_c = 40\%$ and for PETG with $\lambda = 6.4 : X'_{am} = 72\%$ and $X_c = 3.5\%$). It follows that a part of the amorphous phase does not participate in glass transition. This part of the amorphous phase considered as a 'rigid amorphous phase' must be taken into account as the third element of a three phase model such as: $X_{am} + X_c + X_{ar} = 100$ with X_{ar} describes the contribution of the rigid amorphous fraction. The variations of X_{ar} versus λ are shown in Fig. 13 for the glass transitions ($X_{ar} = 100 - X_{am} - X_c$ with X_{am} determined from DSC data) and for the secondary relaxation process ($X_{ar} = 100 - X'_{am} - X_c$ with X'_{am} determined from TSDC data).

For the lowest draw ratio ($\lambda < 2$), the drawing induces in PET only a weak orientation of the macromolecules in the drawing direction. This weak orientation, too small to modify the glass transition (temperature and width), is sufficient to modify the birefringence and the thermal recrystallisation of the initial amorphous sample. No rigid amorphous fraction could be attributed to the drawing. Between $\lambda = 2$ and $\lambda = 4$, the strain induced crystalline phase which appears in the sample is accompanied with a rigid amorphous fraction. This fraction is probably linked to the crystallites, which can explain its low mobility and the disappearance of cooperative motions associated with the glass transition. Nevertheless, contrary to what happens in the crystalline phase, localised motions are possible in the rigid amorphous fraction. The remaining amorphous phase is also perturbed in itself even relaxations are possible. When the draw ratio increases, this phase becomes more heterogeneous. For the highest draw ratio ($\lambda > 4$), the crystalline and the rigid amorphous phases have reached their maximum, and macromolecules are oriented in the drawing direction.

For weakly drawn PETG samples ($\lambda < 4.5$), no crystallites exist and the degree of rigid amorphous fraction is low and close to 7%. This value is too close to the domain of uncertainty domain to conclude that such a rigid amorphous fraction exists. The drawing probably oriented the macromolecules without important modification of the amorphous phase. For $\lambda > 4.5$, a strain induced crystalline phase appears but its percentage is weak ($\approx 3.5\%$). Nevertheless, an important increase of the rigid amorphous fraction occurs and reaches 25% for the highest draw ratio. This seems to indicate that the crystallites act as nucleus for the appearance of the rigid amorphous fraction. No modification of the homogeneity of the remaining amorphous phase is observed. The β relaxation is permitted, as in PET, in the whole amorphous fraction ($X_{ar} + X_{am}$).

5. Conclusions

In this work, we have shown that a rigid amorphous fraction can appear in drawn polyester. This amorphous fraction is enhanced by the presence of strain-induced crystallites. To conclude on the respective influence of the drawing and of the crystalline phase on the non-crystalline part of the material, this is the presence of crystallites in drawn polyesters which is the major factor increasing the degree of rigid amorphous fraction. In this fraction, cooperative motions are forbidden but local motions are allowed as in the mobile amorphous phase. The amorphous phase is also perturbed and becomes less homogeneous when its percentage is low (PET $\lambda > 4$).

References

[1] Li Y, Xue G. Polymer 1999;40:3165.
[2] Seyler RJ. J Therm Anal 1997;49:491.
[3] Coburn JC, Boyd RH. Macromolecules 1986;19:2238.
[4] Cheng SZD, Cao MY, Wunderlich B. Macromolecules 1986;19:1868.
[5] Mathot VBF. Thermal characterization of states of matter. In: Mathot VBF, editor. Calorimetry and thermal analysis of polymers. Munich: Hanser, 1994. p. 105.
[6] Huo P, Cebe P. J Polym Sci Polym Phys 1992;30:239.
[7] Bouriot P, Jacquemart J, Sotton M. Bull Sci ITF 1977;6:9.
[8] Hagege R, Mamy C, Thiroine C. Makromol Chem 1978;179:1069–81.
[9] Dargent E, Grenet J, Auvray X. J Therm Anal 1994;41:1409.
[10] Dargent E, Grenet J, Dahoun A. Polym Engng Sci 1997;37:1853–7.
[11] Kattan M, Dargent E, Ledru J, Grenet J. J Appl Polym Sci 2001;81:3405–12.
[12] Van Turnhout J. Thermally stimulated discharge of polymer electrets. Amsterdam: Elsevier, 1975.
[13] Sauer BB, Avakian P. Polymer 1992;33:5128.
[14] Laredo E, Grimau M, Müller A, Bello A, Suarez N. J Polym Sci Polym Phys 1996;34:2863.
[15] Lacabanne C, Lamure A, Teyssedre G, Bernes A, Mourgues-Martin M. J Non-Cryst Solids 1994;172–174:884.
[16] Santais JJ. CNAM Thesis. Rouen France, 1992.
[17] Hay IL. In: Fava RA, editor. Methods of experimental physics, vol. 16. New York: Academic Press, 1980. p. 163 part C.
[18] Konda A, Nose K, Ishikawa H. J Polym Sci A2 1976;14:1495.
[19] Gupta VB, Kumar S. J Polym Sci Polym Phys 1979;17:1307.
[20] Devries AJ, Bonnebat C, Beautemps J. J Polym Sci Polym Symp 1977;58:109.
[21] Dumbleton JH. J Polym Sci A2 1968;6:795.
[22] Schwach E. Unpublished results.
[23] Bernes A, Martin M, Martinez JJ, Boye J, Lacabanne C. J Therm Anal 1992;38:169.
[24] Dargent E, Santais JJ, Saiter JM, Bayard J, Grenet J. J Non-Cryst Solids 1994;172:1062–5.
[25] Wunderlich B. Macromolecular physics. New York: Academic Press, 1980.